

Modelling beam-to-column joints in seismic analysis of RC frames

Carmine Lima^{*1}, Enzo Martinelli^{1a}, Lorenzo Macorini^{2b} and Bassam A. Izzuddin^{2c}

¹Department of Civil Engineering, University of Salerno, Via Giovanni Paolo II n. 132, 84084 Fisciano, Italy

²Department of Civil and Environmental Engineering, Imperial College London, South Kensington, London SW7 2AZ, United Kingdom

(Received September 30, 2015, Revised December 2, 2016, Accepted December 3, 2016)

Abstract. Several theoretical and analytical formulations for the prediction of shear strength in reinforced concrete (RC) beam-to-column joints have been recently developed. Some of these predictive models are included in the most recent seismic codes and currently used in practical design. On the other hand, the influence of the stiffness and strength degradations in RC joints on the seismic performance of RC framed buildings has been only marginally studied, and it is generally neglected in practice-oriented seismic analysis. To investigate such influence, this paper proposes a numerical description for representing the cyclic response of RC exterior joints. This is then used in nonlinear numerical simulations of RC frames subjected to earthquake loading. According to the proposed strategy, RC joints are modelled using nonlinear rotational spring elements with strength and stiffness degradations and limited ductility under cyclic loading. The proposed joint model has been firstly calibrated against the results from experimental tests on 12 RC exterior joints. Subsequently, nonlinear static and dynamic analyses have been carried out on two-, three- and four-storey RC frames, which represent realistic existing structures designed according to old standards. The numerical results confirm that the global seismic response of the analysed RC frames is strongly affected by the hysteretic damage in the beam-to-column joints, which determines the failure mode of the frames. This highlights that neglecting the effects of joints damage may potentially lead to non-conservative seismic assessment of existing RC framed structures.

Keywords: RC frames; joints; seismic analysis

1. Introduction

Existing reinforced concrete (RC) frames in seismic zones are generally vulnerable to earthquakes. This is mainly because they were designed and built according to past codes of practice, which do not consider the design principles and structural detailing rules complying with the well-established capacity design philosophy (Paulay and Priestley 1992). In fact, the observation of damage induced to existing RC frames by recent earthquakes clearly highlights their deficiency in satisfying the required level of damage limitation and structural safety (Çelebi *et al.* 2010).

Although beam-to-column joints are often considered among the most critical components in existing RC frames (Lu *et al.* 2012), their local response and progressive damage under seismic-induced cyclic loading is generally neglected in practice-oriented analyses. These are usually carried out employing models where beam and column elements are rigidly connected at the joints potentially leading to overestimating the seismic performance of the frames.

In spite of this general lack of attention to the behaviour of the joints in practical seismic assessment of RC frames, the joint response was extensively studied in the last four decades (Zhou and Zhang 2012, Xing *et al.* 2013), and several capacity models for evaluating the shear strength under monotonic loading have been proposed in the scientific literature (Kim and LaFave 2007). A thorough overview of these models was presented and discussed by Lima (2012), providing a systematic assessment of their predictive capacity, based on comparisons against available experimental results. It was pointed out (Lima *et al.* 2012a) that most of current capacity models for RC joints, owing to their mostly empirical nature resulting from the calibration against specific sets of experimental results, guarantee different level of accuracy when predicting the resistance of different kinds of joints (i.e., unreinforced, under-reinforced or EC8-compliant (Chun 2014)). Recently, additional models (Park and Mosalam 2009) were developed not only for determining the ultimate capacity of RC joints, but also for describing the evolution of their response under cyclic actions.

The first attempt to simulate the cyclic response of beam-column joints is due to Giberson (1969), who proposed a numerical description utilising elastic beam-column elements for beams and columns and allowing for the inelastic response of the joints and the nonlinear flexural behaviour of the concrete members by adopting two nonlinear rotational springs at the end of each elastic beam-column element. A different approach was put forward by Alath and Kunnath (1995) who developed the so-called Scissor Model, where the relative rotational deformation

*Corresponding author, Ph.D.

E-mail: clima@unisa.it

^aAssociate Professor

E-mail: e.martinelli@unisa.it

^bLecturer, Ph.D.

E-mail: l.macorini@imperial.ac.uk

^cProfessor

E-mail: b.izzuddin@imperial.ac.uk

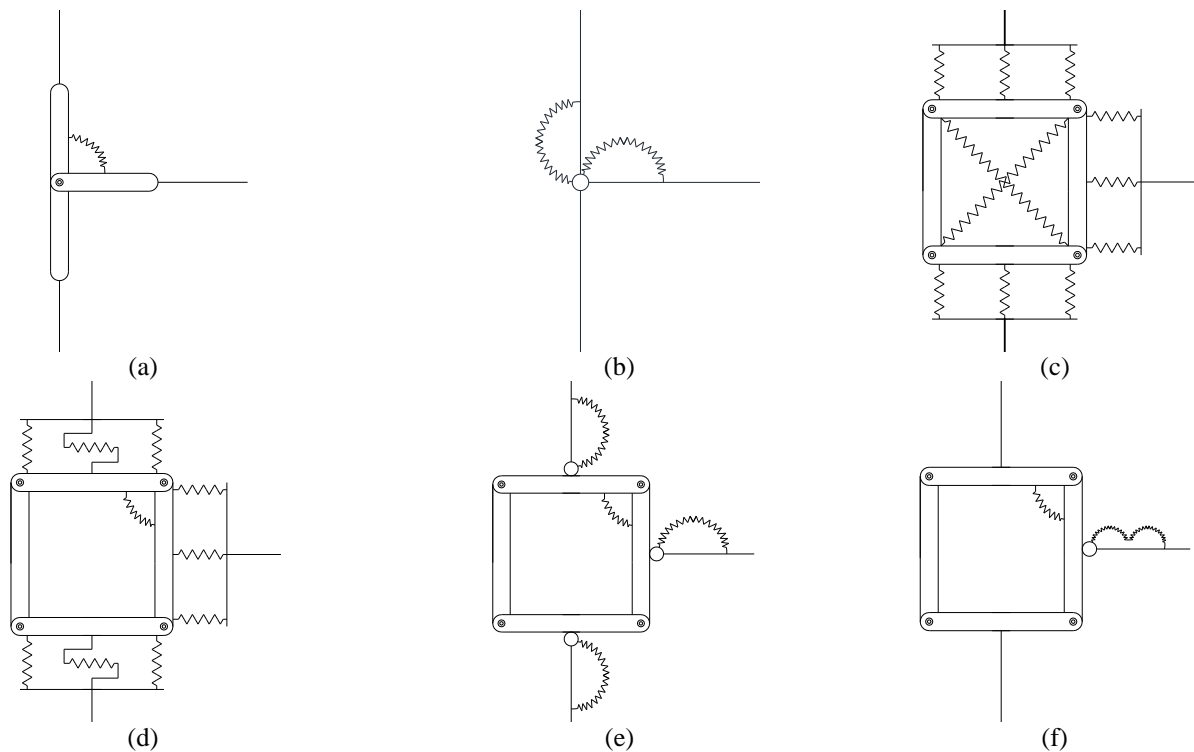


Fig. 1 Models to simulate the cyclic response of exterior joints

between the beam and the column was controlled by a zero-length rotational spring element calibrated against experimental results (see Fig. 1(a)). Later on, Biddah and Ghobarah (1999) modified the model by Alath and Kunnath (1995) employing an additional rotational spring element to include the effect of the bond slip (see Fig. 1(b)). The shear stress-strain relationship was assumed trilinear based on the softened truss model theory (Hsu 1993). A more refined but rather complex model was then presented by Youssef and Ghobarah (2001). This was based on using nine translational springs to simulate the inelastic behaviour due to bond-slip and concrete crushing, and two diagonal axial springs to describe the joint shear deformation (see Fig. 1(c)). Lowes and Altoontash (2003) and Mitra and Lowes (2007) developed a frame model using nine translation springs, similar to the one proposed by Youssef and Ghobarah (2001), in which a rotational spring replaced the two diagonal springs for simulating joint shear distortion (see Fig. 1(d)). The model by Lowes and Altoontash (2003) is based upon the modified compression field theory (MCFT) developed by Vecchio and Collins (1986) for deriving the moment-rotation relationships of the joint panel. The model by Mitra and Lowes (2007) considers a diagonal concrete strut allowing for the confinement exerted by the transverse hoops within the joints which utilises the constitutive model for confined concrete developed by Mander *et al.* (1988). A simplification of the model by Lowes and Altoontash (2003) was proposed by Altoontash and Deierlein (2003) in which three rotational springs replaced the nine translational springs (see Fig. 1(e)). Finally, Shin and LaFave (2004) assembled four rigid frames for representing the joint panel and one rotational spring was located at one of the four hinges; two additional

rotational springs were located in series between the beam and the joint for simulating bond-slip and inelastic rotation (see Fig. 1(f)).

Some attempts to investigating the influence of the local behaviour of beam-column joints on the seismic response of RC frames using some of the aforementioned models were made by Ghobarah and Biddah (1999), Calvi *et al.* (2002) and Kwak *et al.* (2004). Ghobarah and Biddah (1999) investigated the seismic response of RC frames using joint elements with two rotational springs. Calvi *et al.* (2002) examined the response of three multi-storey frame structures by using a simple analytical Scissor Model for representing the joint behaviour. Finally, Kwak *et al.* (2004) proposed a refined model for the nonlinear dynamic analysis of RC structures which was calibrated against experimental results. Although this model considered the influence of anchorage slip, its skeleton curve did not include a degrading branch.

In any case, it was shown that an accurate prediction of the response of RC frames can be obtained only if suitable mechanical laws representing the joints nonlinear behaviour are employed (Favvata and Karayannis 2014). An accurate phenomenological representation of the nonlinear joint behaviour under monotonic and cyclic can be achieved using the "Pivot model" (Dowel *et al.* 1998) which foresees limited rotational capacity and takes into account both strength and stiffness degradation. In defining the model parameters, reliable values for the joint stiffness and strength are required. As far as the joint stiffness is concerned, analytical models for elastic and post-elastic stiffness were provided by Biddah and Ghobarah (1999), Belarbi and Hsu (1995) and Vecchio and Collins (1986). On the other hand, several empirical and theoretical models

were developed in the past years for predicting joint shear strength (Lima *et al.* 2012b). In particular, the model proposed by Vollum and Newman (1999) provides a simple formulation which allows good and reliable joint strength prediction.

In this work, the seismic performance of existing RC frames was investigated through nonlinear analysis using ADAPTIC (Izzuddin 1991), a finite element program for the analysis of structures under extreme loading conditions. The modelling strategy suggested in Favvata *et al.* (2008), and based on the use of simple single rotational spring elements (Scissor Model) to account for the limited stiffness and strength of exterior beam-column joints was considered. The Pivot models was employed to represent the nonlinear response of the nonlinear rotational springs. Conversely, the deformability and potential damage in internal joints were not considered, assuming that internal connections were confined, and that adequate bar anchorage provided high bond strength for the reinforcement through the joints. Moreover, in the employed modelling approach, geometric nonlinearity and the spread of plasticity trough beam and columns were also taken into account using an elasto-plastic cubic formulation (Izzuddin and Lloyd Smith 2000).

In the first part of the paper, the mechanical law employed for modelling damage in exterior joints is presented, and the calibration of the main model material parameters is discussed. The potential and accuracy of the proposed joint model is validated through numerical-experimental comparisons, considering the behaviour of 12 RC exterior beam-to-column joints under cycling loading. Then, in the second part, the calibrated joints model is used to assess the influence of the local response of beam-to-column joints on the seismic performance of reinforced concrete structures, carrying out static and dynamic nonlinear analyses. Particularly, two-, three- and four-storey plane frames, designed only for gravitational loads (Faella *et al.* 2009) are analysed.

showing the influence of the local behaviour of exterior joints on the global seismic response.

2. Joint modelling

Therefore, this paper is firstly aimed at proposing a possible calibration of the main parameters used within the Pivot Model for modelling joints in existing RC frames. Secondly, the calibrated joint model is employed in nonlinear structural analysis for the vulnerability assessment of typical existing frames with the aim of

According to the model proposed by Favvata *et al.* (2008), the joint panel behaviour was represented through the Scissor model shown in Fig. 2 in which a rotational spring relates the bending moment M to the relative rotation θ between beam and column. The remaining two translational degrees of freedom in the plane of the element nodes, which are connected at the joint, are rigidly linked to each other.

Observations of the experimental behaviour of physical exterior joints under cyclic loading consistently showed that the unloading stiffness decreases as plastic deformation increases. Moreover, upon load reversal, the force-displacement path usually crosses the initial elastic response. Fig. 3 illustrates two typical results of cyclic tests

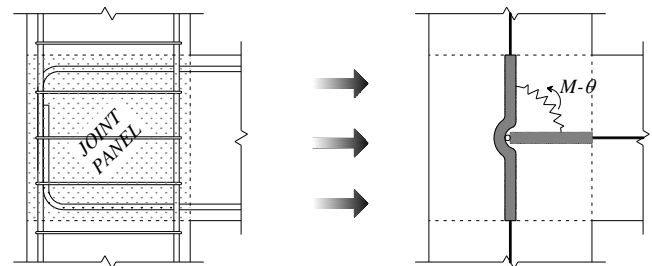
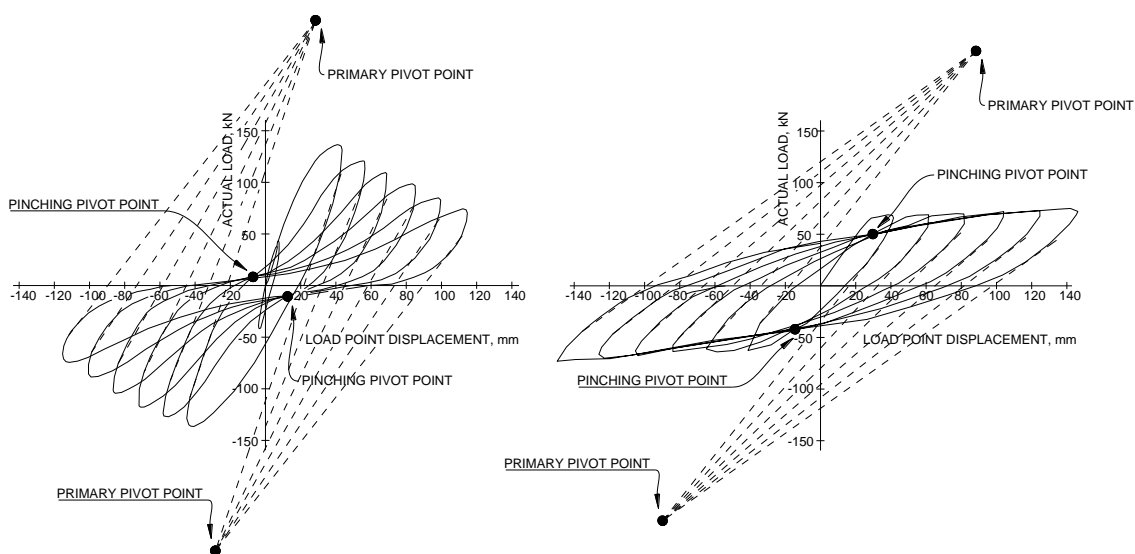


Fig. 2 Idealization of the exterior joint element in frame analysis



(a) Specimen 2B by Ehsani and Wight (1985)

(b) Specimen A by Chutarat and Aboutaha (2003)

Fig. 3 Typical force-displacement behaviour of exterior beam-column joints

on exterior joints. Fig. 3(a) shows the hysteretic behaviour of the exterior joint 2B tested by Ehsani and Wigth (1985) in which high pinching effects were observed. Fig. 3(b) displays the cyclic moment-rotation curve obtained in the experimental test performed by Chutarat and Aboutaha (2003) on an exterior joint in which pinching was not relevant (Favvata and Karayannis 2014).

For both the hysteretic responses shown in Fig. 3, it can be observed that unloading back to zero force from any displacement level is guided toward a single point in the force-displacement plane on the idealised initial stiffness line (Primary Point for the positive and negative branch, respectively). It was also observed that all force-displacement paths tend to cross the elastic loading line at approximately the same point (Pinching Point).

The Pivot model (Dowel *et al.* 1998) which is capable of well reproducing such characteristics was used in this paper for representing the nonlinear behaviour of the joint.

Fig. 4 shows a nonlinear moment-rotation curve drawn according to this model. The monotonic response is asymmetric; elastic and plastic moment $M_{yp(n)}$ and $M_{pp(n)}$ should be defined together with the Pivot Points which allow the determination of the stiffness degradation, caused by the damage evolution in the joint. The Primary Pivot Points P_{1p} , P_{1n} , P_{2p} and P_{2n} control the softening expected by increasing the displacement. Their positions can be determined considering the elastic moments and the amplification parameters α_1 and α_2 . Two moment values $\beta_1 M_{yn}$ and $\beta_2 M_{yp}$ are also defined to define the Pinching Pivot Point for controlling the pinching effect on the cyclic response. Although the Pinching Pivot Points are initially fixed, they move toward the force-displacement origin once strength degradation has occurred (Dowel *et al.* 1998). Three stiffness values $K_{ep(n)}$, $K_{pp(n)}$ and $K_{hp(n)}$ characterise the monotonic laws in the elastic, plastic and hardening phase. Moreover, a multi-parametric strength degradation formulation is used to take in account the reduction of the joint strength according to the Eq. (1) given below (Bella 2009)

$$\Delta M = M_y \cdot \gamma \cdot \left\{ 1 - \left[1 - \left(\frac{E_p}{E_{um} + E_p} \right)^\varepsilon \right] \cdot \left[1 - \left(\frac{\theta_{max}}{\theta_{um}} \right)^\delta \right] \right\} \quad (1)$$

where the coefficients γ , ε and δ are the strength, energy and displacement degradation parameters, E_p is the dissipated energy, E_{um} is the dissipated energy under monotonic loading, θ_{max} is the maximum rotation experienced by the joint in previous cycles, and θ_{um} is the ultimate rotation under monotonic loading.

When using the Pivot model for representing the nonlinear behaviour of the joint, strength and stiffness can be calculated employing specific analytical formulations, while the degradation parameters should be calibrated considering experimental data.

Dowel *et al.* (1998) provided values ranging from 1,50 to 5,00 for α and 0,50 to 0,55 for β , to estimate the degradation parameter derived from specimen tests on circular reinforced concrete column. Moreover, Sivalsevan and Reinhorn (2000) performed a sensitivity analysis for the hysteretic model parameters obtaining the ranges of α and β

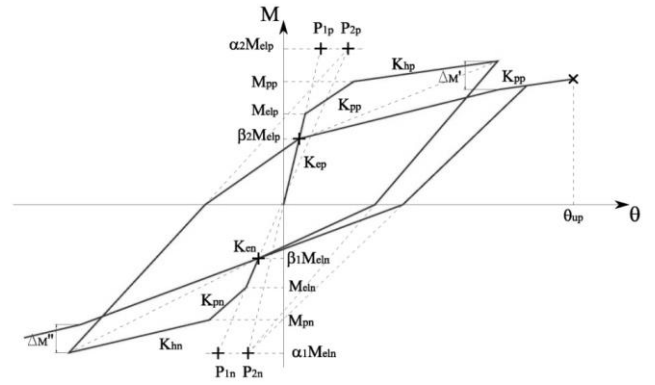


Fig. 4 Pivot model

Table 1 Range of parameters α and β involved in the Pivot Model

Parameter	Controlled effect	Mild	Moderate	Severe
α	Stiffness degradation	15	10	4
β	Pinching	0.15	0.30	0.60

reported in Table 1.

No information was found in the scientific literature about values and the intervals of variation for the parameters γ , ε and δ for the hysteretic model under consideration that control strength, energy and displacement degradation. A possible calibration of these parameters is proposed in Section 3.

2.1 Joint strength model

The model proposed by Vollum and Newman (1999), being very simple but accurate allowing for reliable joint strength predictions (Lima *et al.* 2012a, b), is used in this paper to evaluate the ultimate shear strength for exterior beam-to-column joints. This model is based on an empirical formulation calibrated against a large experimental database incorporating results from many tests reported in the technical literature. According to this model, the shear strength of exterior beam-column joints is determined considering two contributions, the shear strength of the joint without stirrups $V_{c,jh}$ and the tensile strength provided by the stirrups inside the connection $V_{s,jh}$

$$V_{jh} = V_{c,jh} + V_{s,jh} \quad (2)$$

The concrete contribution $V_{c,jh}$ depends on the ultimate strength of the compressed strut which can be evaluated as follows

$$V_{c,jh} = 0.642 \cdot \beta \cdot \left[1 + 0.555 \cdot \left(2 - \frac{h_b}{h_c} \right) \right] \cdot b_j \cdot h_c \cdot \sqrt{f_c} \quad (3)$$

where parameter β is assumed equal to 1.00 for connections with L end-bars and 0.90 for ones with U end-bars bent into panel zone, h_b and h_c represent the depth of the beam and the column, respectively and f_c is the concrete compressive

strength. The effective joint width b_j is conventionally assumed as the average of the beam (b_b) and column (b_c) widths according to the following equation

$$b_j = \begin{cases} \min\left(\frac{b_c + b_b}{2}; b_b + \frac{h_c}{2}\right) & \text{if } b_b \leq b_c \\ \min\left(b_b; b_c + \frac{h_c}{2}\right) & \text{if } b_b > b_c \end{cases} \quad (4)$$

The shear strength provided by the stirrups in the joint can be evaluated as follows

$$V_{s,jh} = A_{w,jh} \cdot f_{sy} - \alpha \cdot b_j \cdot h_c \cdot \sqrt{f_c}, \quad (5)$$

in which $A_{w,jh}$ is the cross-sectional area of the joint stirrups within the top five-eighth of the beam depth, f_{sy} the yielding stress of the joint stirrups and α is a coefficient including the effects of the column axial load, the concrete strength, the amount of stirrups in the panel zone and the joint aspect ratio (conservatively Vollum and Newman (1999) suggest $\alpha=0.2$ [MPa^{0.5}]).

The authors (Vollum and Newman 1999) limited the shear strength V_{jh} of exterior joint to the following upper bound

$$V_{jh} \leq 0.97 \cdot b_j \cdot h_c \cdot \sqrt{f_c} \cdot \left[1 + 0.555 \cdot \left(2 - \frac{h_b}{h_c}\right)\right] \leq 1.33 \cdot b_j \cdot h_c \cdot \sqrt{f_c} \quad (6)$$

based on the assumption that an increment of h_b/h_c leads to a reduction of the shear strength V_{jh} .

Finally, the ultimate moment $M_{pp(n)}$ for the Pivot relationship was evaluated on the basis of the shear strength V_{jh} by means of geometrical conditions. In particular the following equation was used

$$M_{pp(n)} = V_{jh} \cdot (d - d'), \quad (7)$$

in which d' is the thickness of the cover concrete and d is the beam effective depth (evaluated as the beam depth h_b minus the thickness of the cover concrete d').

2.2 Joint stiffness model

The model proposed by Biddah and Ghobarah (1999) was considered for determining the joint stiffness. As it is strongly affected by potential slip of bars throughout the joint, the authors proposed a simple analytical approach for relating the loss of stiffness to the bars slip. The moment-rotation relationship was defined using an elastic-plastic relationship considering the yielding (M_y, θ_y) and ultimate (M_u, θ_u) limits, while neglecting strain hardening (see Fig. 5). This formulation led to evaluate the elastic $K_{ep(n)}$ and plastic $K_{pp(n)}$ stiffness values in both the positive and negative branches which are required by the Pivot relationship. Beyond the ultimate rotation θ_u the hardening stiffness values $K_{hp(n)}$ in the positive and negative branches were taken equal to zero (see Fig. 5).

This model depends on several mechanical parameters evaluated by the authors (Biddah and Ghobarah 1999) on the basis of experimental results. With the aim of taking into account the bond-slip, a parameter L_s was defined as

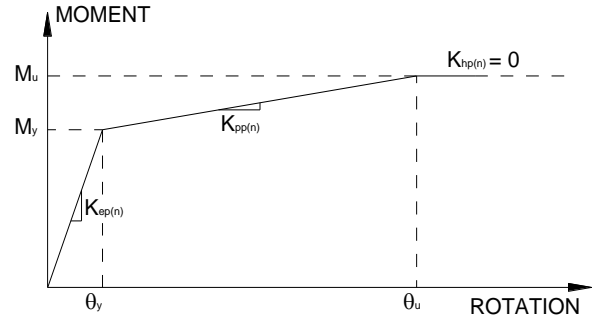


Fig. 5 Moment-rotation relationship idealised

the distance from the beam-column interface to the point in which the longitudinal rebar begins to slip. This parameter depends on the diameter of the bar d_b , the Young's Modulus of the steel rebar and the concrete compressive strength f_c

$$L_s = \frac{E_s \cdot d_b}{2400 \cdot \sqrt{f_c}} \quad (\text{units in } N, mm), \quad (8)$$

The model includes two different formulations in the case of slip onset before or after yielding.

The penetration of yielding into the beam-column connection was denoted by L_y and assumed as a function of the strain hardening of bars χ defined as follows

$$\chi = \frac{f_{us}}{f_{ys}} \rightarrow \begin{cases} \text{for } 1 \leq \chi \leq 1.05 \rightarrow L_y = 2000 \cdot \chi - 2000 \quad (mm), \\ \text{for } 1.05 < \chi \rightarrow L_y = 500 \cdot \chi - 425 \quad (mm) \end{cases} \quad (9)$$

while two upper limit values for the length L_{max} of the slip region and $L_{y,max}$ of the yielding penetration were graphically defined (Biddah and Ghobarah 1999).

The length of the yielding region L_y which should not exceed the maximum limit $L_{y,max}$, can be assumed as $L_s + L_y \leq L_{max}$.

In the first case, when the slip onset occurs before the bar yielding, as the anchorage length L_{max} is smaller than the minimum anchorage length L_s resulting in bars yielding, the initial elastic stiffness $K_{ep(n)}$ and the flexural moment at yielding $M_{elp(n)}$ are given by the following equations

$$K_{ep(n)} = \frac{2 \cdot n \cdot A_s \cdot E_s \cdot (d - d')^2}{L_{max}}, \quad (10)$$

$$M_{elp(n)} = \frac{n \cdot A_s \cdot f_{ys} \cdot (d - d') \cdot L_{max}}{L_s}, \quad (11)$$

in which n and A_s are the number and the cross section area of reinforcing bars in the beam, E_s and f_{ys} are the Young's Modulus and the yielding stress of the steel bars and d is the beam effective depth (evaluated as the beam depth h_b minus the thickness of the cover concrete d'). After bond slip the behaviour is perfectly plastic ($K_{pp(n)}=0$) and $M_{up(n)}$ is taken equal to $M_{elp(n)}$.

Conversely, when the bar yielding occurs before slippage ($L_{max} > L_s$), the stiffness $K_{ep(n)}$ of the elastic branch and the yielding moment $M_{elp(n)}$ are evaluated as follows

$$K_{ep(n)} = 1200 \cdot \pi \cdot n \cdot d_b \cdot (d - d')^2 \cdot \sqrt{f_c}, \quad (12)$$

$$M_{elp(n)} = n \cdot A_s \cdot f_{ys} \cdot (d - d'), \quad (13)$$

in which d_b is the diameter of the steel bars in the beam.

After yielding, the stiffness $K_{pp(n)}$ depends on the minimum anchorage length L_s , the maximum length $L_{y,max}$ of the yielded region and the ratio χ_2 between the ultimate moment $M_{up(n)}$ as evaluated at the end of the previous subsection and the yielding one $M_{elp(n)}$ and it is given by

$$K_{pp(n)} = \begin{cases} \frac{2 \cdot (\chi - 1) \cdot n \cdot A_s \cdot (d - d')^2 \cdot E_s}{2 \cdot L_{y,max} + \left(\frac{\chi - 1}{\zeta}\right) \cdot L_{y,max}} & (\text{if } L_s + L_{y,max} \leq L_{max}), \\ \frac{2 \cdot (\chi - 1) \cdot n \cdot A_s \cdot (d - d')^2 \cdot E_s}{(L_{max} - L_s) + \left[2 + \left(\frac{\chi - 1}{\zeta}\right)\right]} & (\text{if } L_s + L_{y,max} > L_{max} \text{ then } L_y = L_{max} - L_s). \end{cases} \quad (14)$$

Further details on the model can be found in Biddah and Ghobarah (1999).

3. Calibration of model parameters

In this work, 12 tests on sub-assemblages (Table 2) representing exterior RC joints analysed under cyclic loading conditions were considered. The original names assigned by the authors to the experimental specimens were changed in this work for sake of clarity.

The nonlinear model was implemented in ADAPTIC (Izzuddin 1991) an advanced program for nonlinear static and dynamic analysis of structures, which incorporates the Pivot model for nonlinear joint elements. To represent exterior joints, the Scissor model was employed and a zero-length rotational spring element connecting two nodes with the same coordinate was adopted, additionally rigid links were considered to describe the portions of the beam and column inside the joint panel as shown in Fig. 2. Beam elements accounting for both material and geometric nonlinearity were used for representing the spread of plasticity along beams and columns. Stiffness and strength were evaluated as explained above using Biddah and Ghobarah (1999) and Vollum and Newman (1999)

formulations respectively. Table 3 reports the values of the stiffness $K_{ep(n)}$ and $K_{pp(n)}$ together with the yielding flexural strength $M_{elp(n)}$ and ultimate moment $M_{up(n)}$ evaluated for the joints under consideration at the positive (p) and negative (n) branch respectively. After reaching the ultimate moment $M_{up(n)}$, an indefinite perfectly plastic branch was considered assuming the hardening stiffness $K_{hp(n)}$ equal to zero.

Since in the majority of the specimens the beam was reinforced symmetrically with identical top and bottom longitudinal reinforcing bars, the stiffness and strength values in the negative and positive branch are also coincident. Only the specimens T1 and T2 corresponding to the specimens JC-1 and JC-2 in Chun and Kim (2004) were different, as the top longitudinal reinforcement in the beam was greater than the bottom one resulting in higher strength in the negative branch. Moreover, according to the formulation of Biddah and Ghobarah (1999) outlined before, in specimens T7 and T11 the bar slip develops before the yielding leading to zero stiffness $M_{pp(n)}$ for the

Table 2 Database for exterior beam-to-column joints under cyclic loading

Authors (year)	Original name of specimens	Name assigned in this paper
Chun and Kim (2004)	JC-1	T1
	JC-2	T2
Hwang <i>et al.</i> (2004)	28-0T0	T3
Chutarat and Aboutaha (2003)	1	T4
	A	T5
Clyde <i>et al.</i> (2000)	Test #4	T6
	Test #5	T7
Economou <i>et al.</i> (1998)	A5	T8
Ehsani <i>et al.</i> (1987)	1	T9
	2	T10
Ehsani and Wigth (1985)	1B	T11
	2B	T12

Table 3 Strength and stiffness assumed for Pivot model in the analysed specimens (units in kNm)

Specimen	Positive branch				Negative branch			
	K_{ep}	K_{pp}	M_{elp}	M_{up}	K_{en}	K_{pn}	M_{eln}	M_{un}
T1	296 000	2 600	174.00	327.00	395 000	3 440	-232.00	-385.00
T2	585 000	5 130	347.00	499.00	780 000	6 750	-463.00	-615.00
T3	388 000	8 260	418.00	584.00	388 000	8 260	-418.00	-584.00
T4	418 000	11 400	389.00	457.00	418 000	11 400	-389.00	-457.00
T5	281 000	1 510	152.00	292.00	281 000	1 510	-152.00	-292.00
T6	332 000	5 900	406.00	411.00	332 000	5 900	-406.00	-411.00
T7	315 000	-	406.00	406.00	315 000	-	-406.00	-406.00
T8	12 300	176	11.30	17.20	12 300	176	-11.30	-17.20
T9	495 000	3 020	199.00	221.00	495 000	3 020	-199.00	-221.00
T10	547 000	3 860	243.00	265.00	547 000	3 860	-243.00	-265.00
T11	436 000	-	257.00	257.00	436 000	-	-257.00	-257.00
T12	363 000	27 300	233.00	239.00	363 000	27 300	-233.00	-239.00

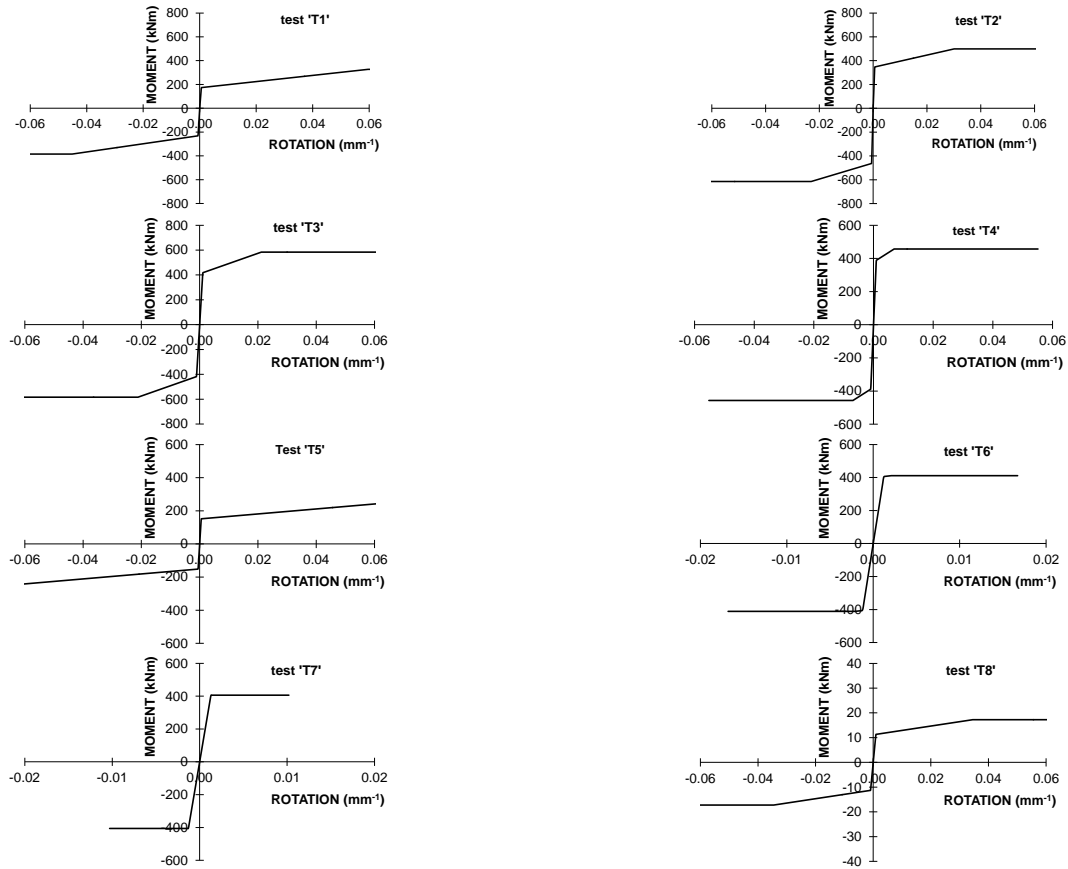


Fig. 6 Curves under monotonic load conditions (tests from T1 to T8)

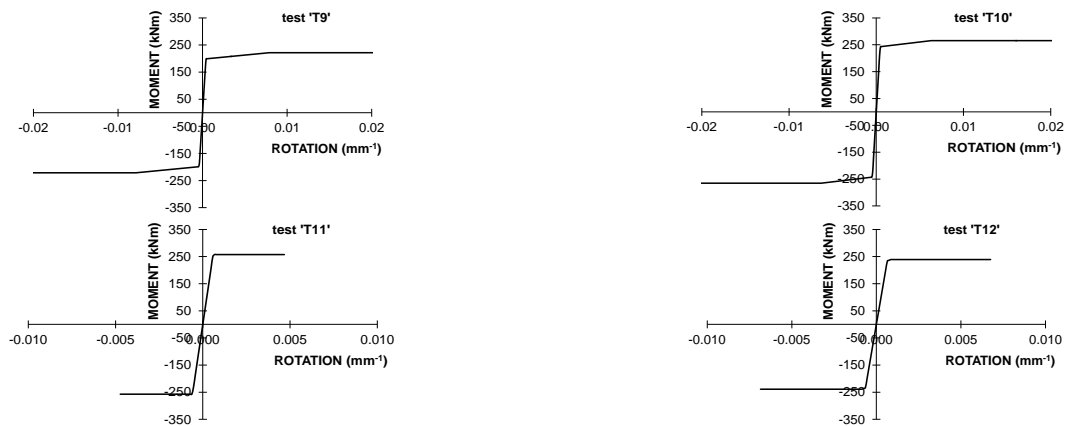


Fig. 7 Curves under monotonic load conditions (tests from T9 to T12)

plastic branch as shown in Figs. 6-7, which displays the nonlinear behaviour under monotonic loading conditions for the 12 experimental tests under investigation obtained from the numerical values listed in Table 3.

The degradation parameters for the Pivot model were derived by calibrating the model against the experimental data. In particular, a number of numerical simulations were carried out changing the degradation parameters. Then the numerical curves representing the joint behaviour were compared with the experimental results, and the parameters minimising the scatter between the experimental and the numerical behaviour were selected. In particular, it was found that:

- α can be assumed equal to 3.00 for all the exterior joints under investigation;
- β equal to 0.50 in 11 specimens and to 0.30 for the other one;
- the strength degradation parameter γ between 0.00 and 0.80;
- the energy degradation parameter ε equal to 5 for one specimen and 15 in the other cases;
- the displacement degradation parameter δ in the interval between 1.25 and 1.50.

In Fig. 8 and Fig. 9 the numerical-experimental

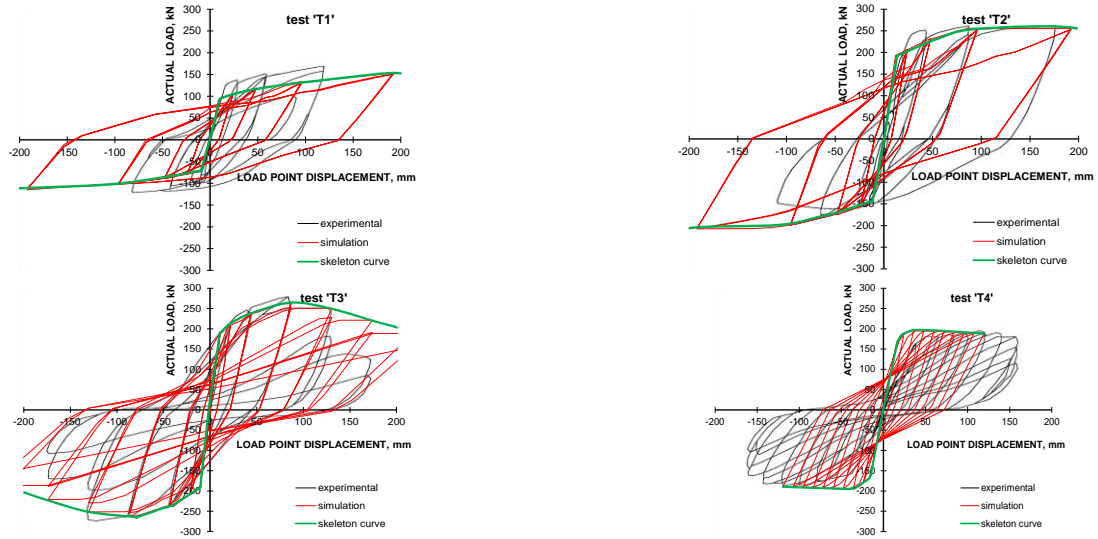


Fig. 8 Comparison between the simulated and observed response (tests from T1 to T4)

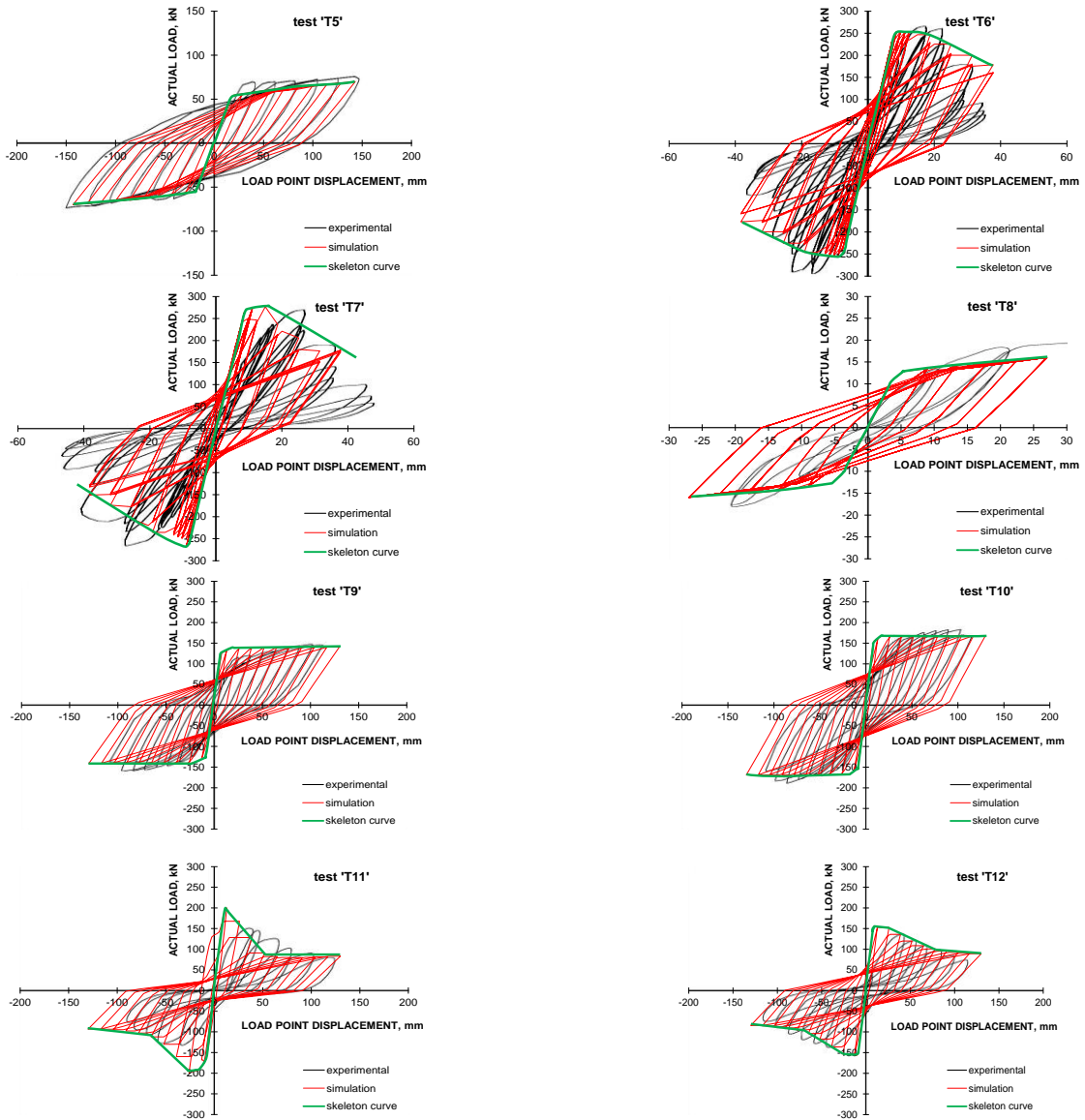


Fig. 9 Comparison between the simulated and observed response (tests from T5 to T12)

comparisons are shown, where the dark lines represent the experimental cyclic response, the red lines indicate the numerical curves and the green curves represent the skeleton curves. These figures show how the calibrated Pivot model can be effectively employed for representing the actual behaviour of external RC joints, both in the case of relevant and negligible pinching effect. Moreover, a good correlation between ultimate experimental strength and the corresponding value calculated using the model by Vollum and Newman (1999) can be observed.

As mentioned before, the Pivot parameters α , β and ε can be assumed constant for exterior joints, in particular $\alpha = 3.00$, $\beta = 0.50$ and $\varepsilon = 15.00$ are suggested herein. A sensitivity analysis was performed to investigate the influence of the Pivot parameters γ and δ , which may vary within a specific interval, with reference to the geometric and mechanical characteristics of the analysed joints. Such an analysis demonstrated that the parameter γ which control the strength degradation is highly influenced by both the amount of horizontal reinforcement in the panel zone and the shear capacity of the joint (see Fig. 10).

As shown in Fig. 10, the parameter γ resulted in a linear log-normal correlation with the area of stirrups inside the joint panel. The parameter γ decreases by increasing the amount of horizontal reinforcement showing that the strength degradation is less relevant in joints with high amount of shear reinforcement. Moreover, the parameter δ controlling the displacement degradation (see Eq. (1)) under cyclic loading was found dependent from the concrete strength (see Fig. 11) and a specific relationship which determines a reduction of δ for an increment in concrete was defined.

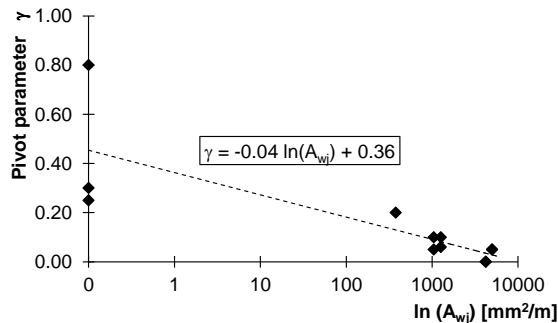


Fig. 10 Dependence of γ on the amount of stirrups in the joint

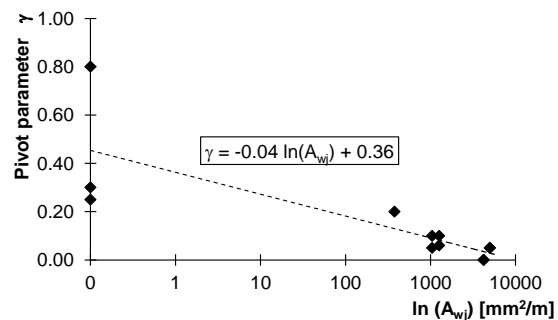


Fig. 11 Dependence of δ on the concrete compressive strength

4. Numerical analysis of multi-storey RC frames

With the aim of evaluating the influence of the nonlinear behaviour of exterior beam-to-column joints on the response of RC frames, numerical nonlinear static and dynamic analyses were carried out using ADAPTIC (Izzuddin 1991), and the seismic vulnerability of the analysed frames was determined. Nonlinear rotational springs were included in frame models for investigating the seismic performance of four-, three- and two-storey plane frame structures with three bays. The analysed frames are parts of realistic structures representative of existing school and hospital buildings built in Italy around the 1960's and 1970's (Faella *et al.* 2009). The mechanical and geometrical characteristics (e.g., amount of reinforcement etc.) of the analysed structures were derived by simulated design according to old codes (Regio Decreto 1939) and standards of practice (Santarella 1963) in force in Italy at the time of construction.

Fig. 12 shows the characteristics of the structure which the plane frames analysed in this study are parts of. In particular, the plane frame in the x -direction related to the alignment of column 5-6-7-8 (namely the 2x plane frame) was investigated. Furthermore, Fig. 12 illustrates a typical section of the floor of the building and presents a table reporting the gravitation loads applied to the structures.

Table 4 and Table 5, with reference to the analysed 2x plane frame report the geometric characteristics of the columns and beams, respectively, in which B is the width of the section and H the height. About the columns, the dimension B is considered along the y -direction and H in the x -direction. Moreover, A_{long} denotes the number and the diameter of the total longitudinal reinforcement in the columns, while A_{sup} and A_{inf} indicate the flexural reinforcement of the beams at top and bottom.

Table 4 Cross section and longitudinal reinforcement of the columns

Section	B [mm]	H [mm]	A_{long}
101	300	300	4 \varnothing 16
102	300	400	4 \varnothing 16 + 2 \varnothing 12
103	400	300	4 \varnothing 16 + 2 \varnothing 12
104	500	300	6 \varnothing 16

Table 5 Cross section and longitudinal reinforcement of the beams

Section	B [mm]	H [mm]	A_{sup}	A_{inf}
1	300	600	3 \varnothing 16	2 \varnothing 16
2	300	600	2 \varnothing 16	5 \varnothing 16 + 1 \varnothing 20
3	300	600	2 \varnothing 16	2 \varnothing 16
4	300	600	4 \varnothing 16	2 \varnothing 16
5	300	500	3 \varnothing 16	2 \varnothing 16
6	300	500	2 \varnothing 16	5 \varnothing 16
7	300	500	7 \varnothing 16	2 \varnothing 16
8	300	500	2 \varnothing 16	3 \varnothing 16

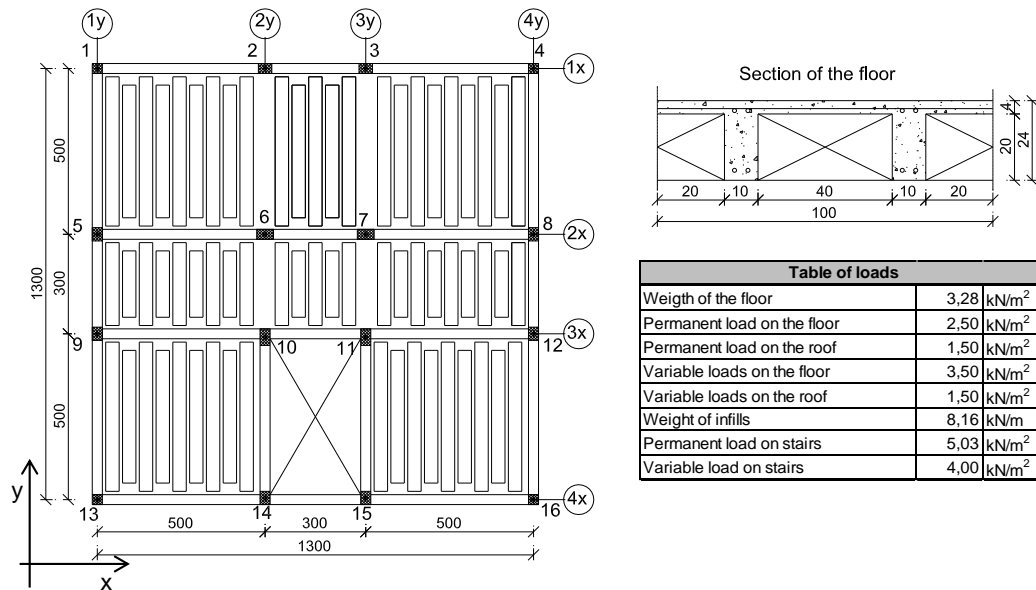


Fig. 12 Structures considered in the analysis

Table 6 Assignment of the column section

Column	1 st storey	2 nd storey	3 rd storey	4 th storey
5	102	101	101	101
6	104	103	101	101
7	104	103	101	101
8	102	101	101	101

Table 7 Assignment of the beam section

Alignment	1y	1 st bay	2y	2 nd bay	3y	3 rd bay	4y
Roof floor	5	6	7	8	7	5	6
Intermediate floor	1	2	4	3	4	2	1

The shear reinforcement in the columns consisted of horizontal stirrups $\Phi 8$ with 200 mm spacing, while beams were reinforced with $\Phi 8$ stirrups spaced 150 mm at the ends and 250 mm in the middle.

The assignment of the cross sections reported in Table 4 and Table 5 to the columns and beams of the four-storey plane frame under investigation based on the numeration shown in Fig. 12 is reported in Table 6 and Table 7. On the other hand, the three-storey frame was obtained as a sub-structure of the four-storey frame by eliminating the first storey. In the same way, the first and the second storeys were removed from the original structure to form the two-storey plane frame.

Typical materials properties used in 1960s and 1970s in Italy were taken into account. Concrete class R_{ck} 25 MPa (cylindrical compressive strength $f_c=28$ MPa) and steel bars AQ42 type (yielding stress $f_y=320$ MPa) were used. The effect of the confinement provided by stirrups was considered for the concrete constitutive law in compression; thus, the compressive strength and the ultimate strain of the concrete core were increased according to the relationship suggested by Paulay and Priestley (1992). The adopted material properties are reported in Table 8.

Table 8 Mechanical characteristics of materials

Cover concrete	Core concrete (confined)	Steel bars
Compressive strength $f_c=28.00$ MPa	Compressive strength $f_{cc}=33.55$ MPa	Yielding stress $f_y=320$ MPa
Strain at yielding $\epsilon_{c0}=0.0020$	Strain at yielding $\epsilon_{c0}=0.0037$	Young's Modulus $E_s=210\,000$ MPa
Ultimate compressive strength $f_{cu}=5.75$ MPa	Ultimate compressive strength $f_{cu}=6.75$ MPa	Hardening ratio 1.00%
Ultimate strain $\epsilon_{cu}=0.0060$	Ultimate strain $\epsilon_{cu}=0.0157$	

In all the examined cases, exterior joints were considered without shear reinforcement and were modelled using the Scissor model with the Pivot law discussed and validated before. As suggested in the previous section the following Pivot parameters were used: $\alpha=3.00$, $\beta=0.50$, $\gamma=0.30$, $\delta=1.50$ and $\epsilon=15$.

Interior joints were considered here as rigid. Although interior joints are not expected to be as vulnerable as the exterior ones, some cracking would normally occur. However as pointed out in previous studies (Favvata *et al.* 2008), the influence of the damage in the interior joints is not expected to be significant for the overall response of the examined frame systems.

4.1 Vulnerability comparison using Static Nonlinear Analysis

The vulnerability of the analysed frames was assessed through static nonlinear analyses. Two different force patterns were considered: a uniform pattern with forces proportional to the floor masses and a modal pattern with forces proportional to the masses and to the modal shape. The performance points, evaluated using the N2-Method (Fajfar 1999), were compared with the capacity points, which are function of the Limit States and of the failure mechanism taken in account. In this work, according to

European and Italian codes (Ministerial Decree 2008), flexural and shear mechanisms in beams and columns were considered to define the Limit State of Damage Limitation (SLD) related to a seismic event whose Probability of Exceedance (PoE) is equal to 63% in 50 years, the Limit State of Life Safety (SLV) corresponding to an event with 10% PoE in 50 years, and the Limit State of Near Collapse (SLC) corresponding to an event with 2% PoE in 50 years. The structure was assumed to be located in L'Aquila (long. 13.3944; lat. 42.3660) and 50 years nominal life in class of use III ($c_u=1.5$) as prescribed by the Ministerial Decree (2008) for school and hospital structures were considered. Table 9 reports the key parameters of the seismic action in which a soil type B and a stratigraphic class T2 (Ministerial Decree 2008) were considered. Fig. 13 shows the Acceleration Displacement Response Spectra (ADRS) of the seismic input for the three Limit States under consideration.

In Fig. 14 the capacity curves determined either considering the joint damage through nonlinear springs (red lines) or assuming rigid and resistant joints (black lines) are compared to highlight the influence of the exterior joint behaviour on the frame seismic performance. The capacity curves calculated considering the two force patterns are shown together with specific performance points, which reveal when the first element exceeds shear or rotational capacity at each Limit State. In this work the chord rotation was assumed as control parameter to define when the three Limit States are reached, and the values of the chord rotation capacities were evaluated according to Eurocode 8 (EN 1998-3 2005).

The use of a nonlinear rotational spring for representing the actual behaviour of exterior joint not only determines a lower initial stiffness for the frames, but, most importantly, it leads to a significant change in the failure mode (Fig. 14). In the analysis of the frame with rigid joints, a floor mechanism characterises the collapse of the structures, conversely a global mechanism determines the performance of the frames modelled accounting for the damage in the joints.

Table 9 Parameters of the seismic induced action

Limit State		SLD	SLV	SLC
Return Period	T_R	75 years	712 years	1462 years
Peak ground acceleration	a_g	0.125 g	0.300 g	0.381 g
Dynamic amplification	F_0	2.316	2.384	2.425
Period at constant velocity	T_C^*	0.290 s	0.356 s	0.373 s
Stratigraphic amplification	S_S	1.200	1.114	1.030
Coefficient of soil	C_C	1.409	1.352	1.340
Coefficient of site	S	1.440	1.337	1.236
Period	T_B	0.136 s	0.161 s	0.166 s
Period	T_C	0.409 s	0.482 s	0.499 s
Period	T_D	2.100 s	2.799 s	3.124 s

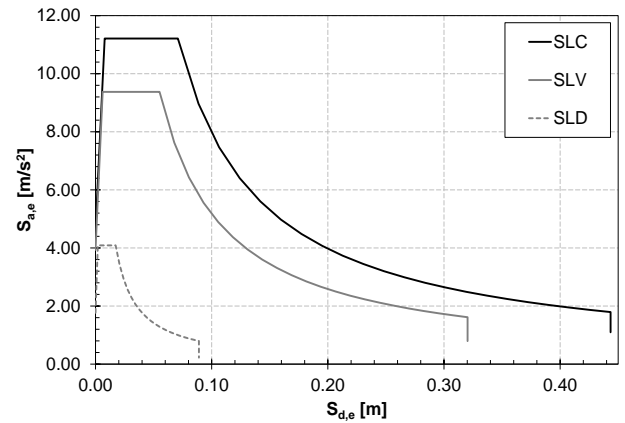


Fig. 13 Elastic spectra in ADRS format

The N2-Method (Fajfar 1999) was used to assess the seismic vulnerability of the analysed frames through the risk index α (Faella *et al.* 2009) defined as the capacity/demand ratio in terms of Peak Ground Acceleration PGA (OPCM 3362 2004)

$$\alpha_u = \min \left\{ \frac{PGA_{SLV}}{PGA_{10\%}}, \frac{PGA_{SLC}}{PGA_{2\%}} \right\}, \quad (15)$$

$$\alpha_e = \frac{PGA_{SLD}}{PGA_{50\%}}, \quad (16)$$

in which PGA_{LS} is the peak ground acceleration resulting in the structure to attain a LS and PGA_{PoE} characterises the design spectra for the given LS and the corresponding PoE.

As shown in Eqs. (15) and (16) two risk index can be defined: the risk index of collapse α_u related to the overlapping on the SLV or SLC and the risk index of inability related to the overlap of service conditions SLD.

If $\alpha \geq 1$, the structure complies with the performance objectives required by the seismic code otherwise it is vulnerable to the considered seismic event. In this paper four values of the risk index α were derived considering, respectively, the three chord rotation limits suggested by the code (EN 1998-3 2005) for the three Limit States under investigation and the shear capacity assumed as a further limitation for SLV.

In Fig. 15, the vulnerability of the frames determined using the two different models, either accounting for the nonlinear joint behaviour (Uniform_J and Modal_J indicate with the grey and thin dashed histograms, respectively) or assuming rigid and resistant joints (Uniform and Modal indicate with the dark and thick dashed histograms, respectively), is compared. The former modelling approach leads to higher α values and therefore lower vulnerability in assessing flexural mechanisms, but higher vulnerability values were obtained when considering brittle failure related to the overlapping of the shear capacity in beams and columns. The lower vulnerability gained at SLV and SLC, when using frame models accounting for joint damage, is due to the lower ductility demand for beams and columns caused by the joint deformability. A more limited reduction in vulnerability is obtained at SLD because the

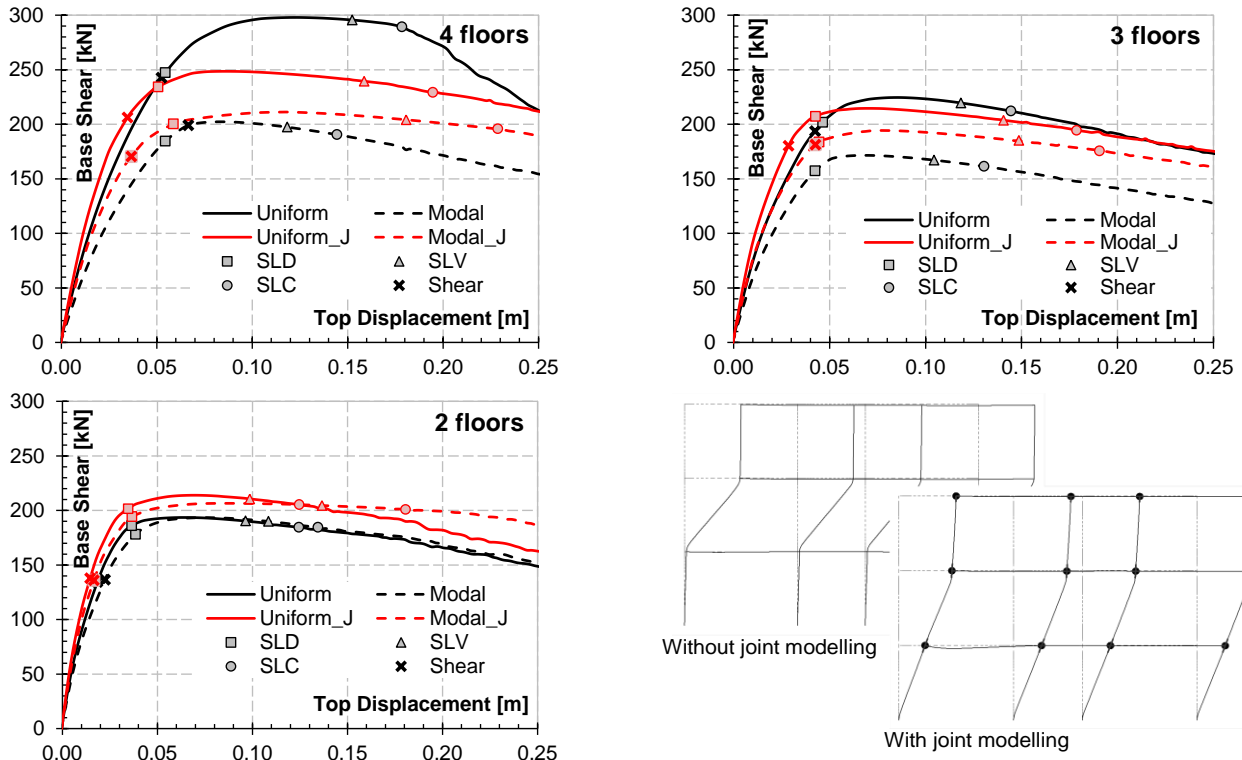


Fig. 14 Capacity curves with performance points and deformed shapes at collapse of the three-storey frame

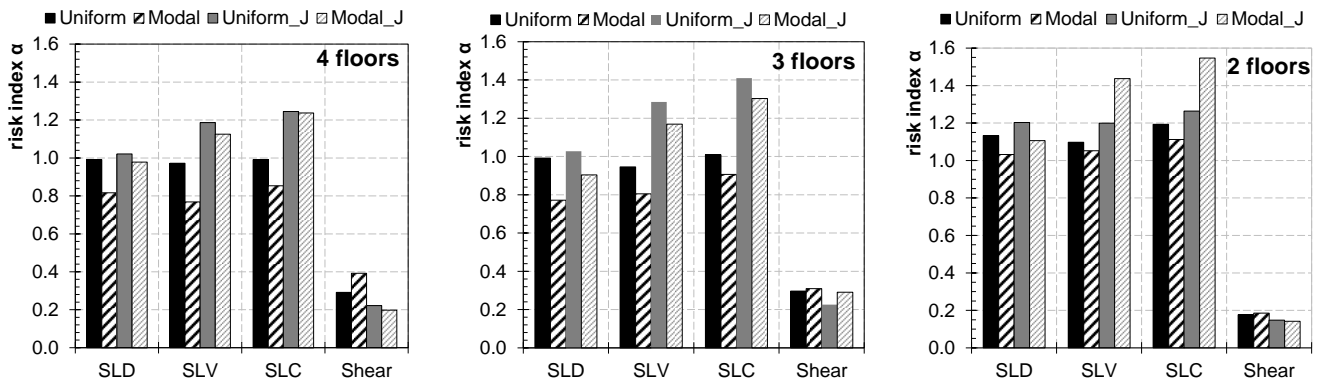


Fig. 15 Vulnerability parameter α at different limit states, considering flexural and shear failure mechanisms

performance at that limit state is not associated with the ductility capacity but with the stiffness of the analysed structure.

4.2 Dynamic nonlinear analysis

The effects of the local response of the exterior joints with reduced capacity on the seismic behaviour of four-, three- and two-storey frame structures were also dynamically investigated by Nonlinear Time History (NLTH) analyses considering the earthquake ground motion recorded at El Centro (1940) as seismic input. Again, the response of the multi-storey frame structures was analysed considering two models, either accounting for the external joint damage or assuming rigid and resistant joints.

The outcomes of the analyses presented in Fig. 16 show limited difference in the top displacements, while

significant variation is observed in inter-storey drift, especially for the two-storey frame. Smaller inter-storey drifts were determined using frame models with nonlinear springs for representing the deformability and damage in exterior joints. Such a result confirms the change in the failure mode already observed in Nonlinear Static Analyses (Fig. 14).

5. Conclusions

The seismic performance of existing RC frames has been investigated accounting for the damage in exterior RC beam-to-column joints, where a scissor nonlinear single-spring model based on the Pivot law has been employed for representing the nonlinear joint behaviour. The parameters of the Pivot model have been determined through a

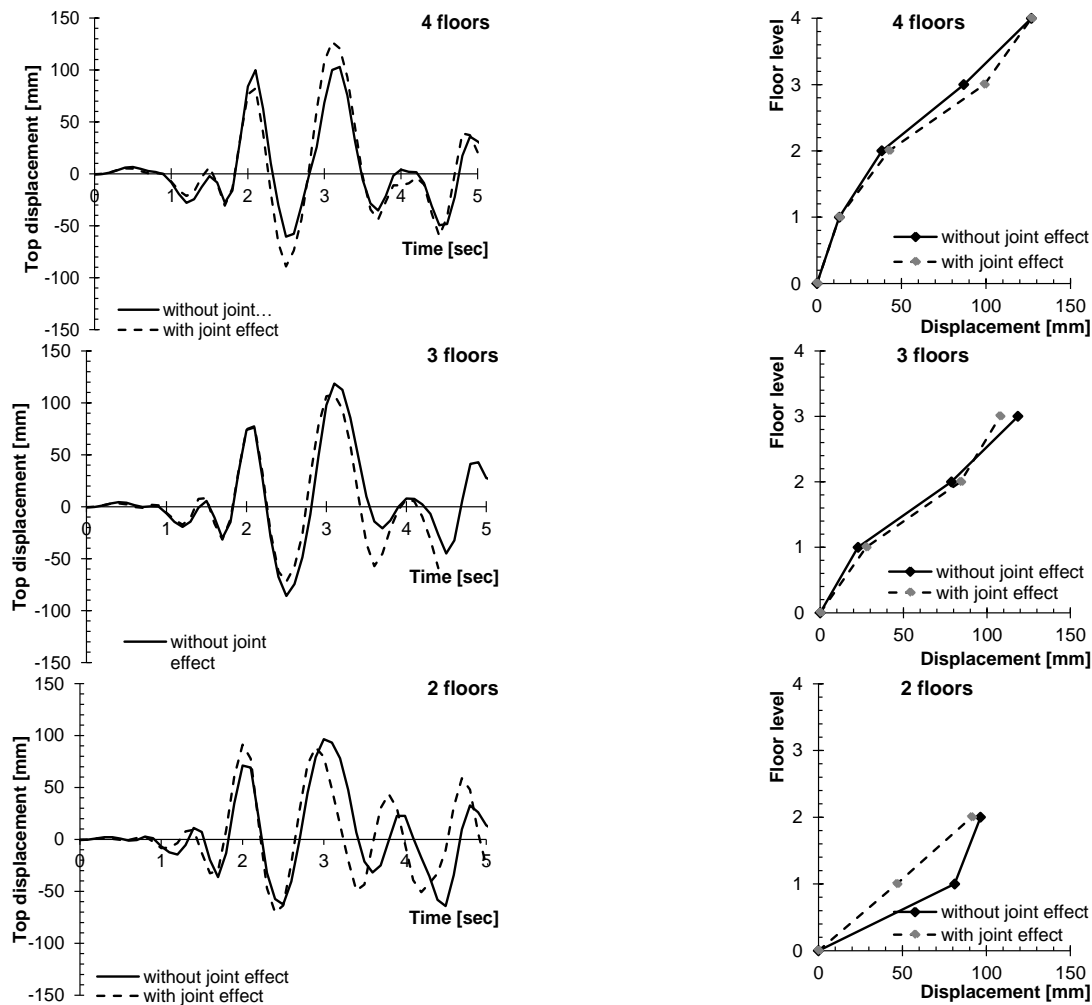


Fig. 16 Top displacement and inter-storey drifts determined through nonlinear dynamic analysis

calibration of numerical simulations against the results of 12 cyclic tests on RC sub-assemblages. It has been observed that some Pivot parameters do not depend on the geometry and mechanical properties of the analysed joints; consequently, these values may be employed in general analysis of existing frames. Moreover, for the parameters which depend on the joints characteristics, a possible correlation with the key joint parameters was proposed: this is the first and most general contribution as correlation for these parameters is not currently available in the scientific literature.

The outcomes of nonlinear static and dynamic analyses, carried out on all the structures assuming either rigid joints or nonlinear springs for exterior joints, reveal that:

- the failure mode of the multi-storey RC frames substantially changes from a floor mechanism in the case of models with rigid joints to a global mechanism considering joint damage;
- considering the so-called “ductile” failure modes, the analyses based on models accounting for joint damage led to lower vulnerability values; conversely, non-conservative vulnerability assessment related to “brittle” failure modes generally resulted from neglecting the effects of joints damage;

- no significant variation in the overall frame response under low intensity ground motion has been observed using either model for exterior joints.

References

- Alath, S. and Kunnath, S. (1995), “Modeling inelastic shear deformation in RC beam-column joints”, *Proceedings of the 10th Conference on Engineering Mechanics*, University of Colorado at Boulder CO, 822-825.
- Altoontash, A. and Deierlein, G.G. (2003), “A versatile model for beam-column joints”, *ASCE Structures Congress Proceedings*, Seattle, Washington, USA.
- Belarbi, A. and Hsu, T.T.C. (1995), “Constitutive Laws of Softened Concrete in Biaxial Tension-Compression”, *ACI Struct. J.*, **92**(5), 562-573.
- Bella, M. (2009), “Modellazione Numerica di Strutture Sismoresistenti e Analisi Probabilistica di Tipo Montecarlo (Numerical modelling and probabilistic analysis of seismic resistant structures)”, Ph.D. Thesis, Department of Civil and Environmental Engineering, University of Trieste, Italy.
- Biddah, A. and Ghobarah, A. (1999), “Modelling of shear deformation and bond slip in reinforced concrete joints”, *J. Struct. Eng. Mech.*, **7**(4), 413-432.
- Calvi, G.M., Magenes, G. and Pampanin, S. (2002), “Relevance of

- beam-column joint damage and collapse in RC frame assessment", *J. Earthq. Eng.*, **6**(1), 75-100.
- Çelebi, M., Bazzurro, P., Chiaraluce, L., Clemente, P., Decanini, L., DeSortis, A. and Stephens, C. (2010), "Recorded motions of the 6 April 2009 Mw 6.3 L'Aquila, Italy, earthquake and implications for building structural damage: overview", *Earthq. Spectra*, **26**(3), 651-684.
- Chun, S.C. and Kim, D.Y. (2004), "Evaluation of mechanical anchorage of reinforcement by exterior beam-column joint experiments", *13th World Conference on Earthquake Engineering*, Vancouver, Canada, August.
- Chun, S.C. (2014), "Effects of joint aspect ratio on required transverse reinforcement of exterior joints subjected to cyclic loading", *Earthq. Struct.*, **7**(5), 705-718.
- Chutarat, N. and Aboutaha, R.S. (2003), "Cyclic response of exterior reinforced concrete beam-column joints reinforced with headed bars-experimental investigation", *ACI Struct. J.*, **100**(2), 254-264.
- Clyde, C., Pantelides, C.P. and Reaveley, L.D. (2000), *Performance-based evaluation of exterior reinforced concrete building joints for seismic excitation - PEER Report 2000/05*, Pacific Earthquake Engineering Research Center, University of California, Berkeley.
- Dowel, R.K., Seible, F. and Wilson, E.L. (1998), "Pivot hysteresis model for reinforced concrete members", *ACI Struct. J.*, **95**(S55), 607-617.
- Economou, C.M., Prinou, C., Chalioris, C.E. and Karayannis, C.G. (1998), "Capacity decrease of RC joints due to seismic actions in the curing period", *11th European Conference on Earthquake Engineering*, Balkema, Rotterdam.
- Ehsani, M.R. and Wight, J.K. (1985), "Exterior reinforced concrete beam-to-column connections subjected to earthquake-type loading", *ACI J.*, **82**(4), 492-499.
- Ehsani, M.R., Moussa, A.E. and Vallenilla, C.R. (1987), "Comparison of inelastic behavior of reinforced ordinary and high strength concrete frames", *ACI Struct. J.*, **84**-S17(2), 161-169.
- EN 1998-3 (2005), *Eurocode 8: Design of structures for earthquake resistance - Part 3: Assessment and retrofitting of buildings*, The European Union Per Regulation 305/2011, Directive 98/34/EC, Directive 2004/18/EC.
- Faella, C., Lima, C. and Martinelli, E. (2009), "Definizione e valutazione parametrica di misure di vulnerabilità sismica per edifici esistenti in cemento armato (paper S14.14)", *XIII Convegno ANIDIS*, Bologna, Italy, June.
- Fajfar, P. (1999), "Capacity spectrum method based on inelastic demand spectra", *Earthq. Eng. Struct. Dyn.*, **28**(9), 979-993.
- Favvata, M.J., Izzuddin, B.A. and Karayannis, C.G. (2008), "Modelling exterior beam-column joints for seismic analysis of RC frame structures", *Earthq. Eng. Struct. Dyn.*, **37**(13), 1527-1548.
- Favvata, M.J. and Karayannis, C.G. (2014), "Influence of pinching effect of exterior joints on the seismic behavior of RC frames", *Earthq. Struct.*, **6**(1), 89-110.
- Giberson, M.F. (1969), "Two nonlinear beams with definition of ductility", *J. Struct. Div.*, ASCE, **95**(ST2), 137-157.
- Ghobarah, A. and Biddah, A. (1999), "Dynamic analysis of reinforced concrete frames including joint shear deformation", *J. Eng. Struct.*, **21**(11), 971-987.
- Hsu, T.T.C. (1993), *Unified Theory of Reinforced Concrete*, CRC Press Inc, Boca Raton, FL, USA.
- Hwang, S.J., Lee, H.J. and Wang, K.C. (2004), "Seismic design and detailing of exterior reinforced concrete beam-column joints", *13th World Conference on Earthquake Engineering*, Vancouver, Canada, August.
- Youssef, M. and Ghobarah, A. (2001), "Modeling of RC beam-column joints and structural walls", *J. Earthq. Eng.*, **5**(1), 93-111.
- Izzuddin, B.A. (1991), "Nonlinear dynamic analysis of framed structures", Ph.D. Thesis, Department of Civil Engineering, Imperial College, London.
- Izzuddin, B.A. and Lloyd Smith, D. (2000), "Efficient nonlinear analysis of 3D R/C frames using adaptive techniques", *Comput. Struct.*, **78**(4), 549-573.
- Kim, J. and LaFave J.M. (2007), "Influence parameters for the joint shear behaviour of reinforced concrete (RC) beam-column connections", *Eng. Struct.*, **29**(10), 2523-2539.
- Kwak, H.G., Kim, S.P. and Kim, J.E. (2004), "Nonlinear dynamic analysis of RC frames using cyclic moment-curvature relation", *J. Struct. Eng. Mech.*, **17**(3-4), 357-378.
- Lima, C. (2012), *Beam-to-column joints in RC frames: capacity models and behaviour under seismic actions*, LAP Lambert Academic Publishing, Germany.
- Lima, C., Martinelli, E. and Faella, C. (2012a), "Capacity models for shear strength of exterior joints in RC frames: experimental assessment and recalibration", *Bull. Earthq. Eng.*, **10**(3), 985-1007.
- Lima, C., Martinelli, E. and Faella, C. (2012b), "Capacity models for shear strength of exterior joints in RC frames: state-of-the-art and synoptic examination", *Bull. Earthq. Eng.*, **10**(3), 967-983.
- Lowes, L.N. and Altoontash, A. (2003), "Modeling reinforced-concrete beam-column joints subjected to cycling loading", *J. Struct. Eng.*, ASCE, **129**(12), 1686-1697.
- Lu, X., Urukup, T.H., Li, S. and Lin, F. (2012), "Seismic behavior of interior RC beam-column joints with additional bars under cyclic loading", *Earthq. Struct.*, **3**(1), 37-57.
- Mander, J.B., Priestley, M.J.N. and Park, R. (1988), "Theoretical stress-strain model for confined concrete", *J. Struct. Eng.*, ASCE, **114**(8), 1804-1826.
- Ministerial Decree (2008), *Norme tecniche per le costruzioni*, 14/01/2008. G.U. n°29 del 4/02/2008. (in Italian)
- Mitra, N. and Lowes, L.N. (2007), "Evaluation, calibration, and verification of a reinforced concrete beam-column joint model", *J. Struct. Eng.*, ASCE, **133**(1), 105-120.
- OPCM 3362 (2004), *Modalità di attivazione del Fondo per interventi straordinari della Presidenza del Consiglio dei Ministri, istituito ai sensi dell'art. 32-bis del decreto-legge 30 settembre 2003, n. 269, convertito, con modificazioni, dalla legge 24 novembre 2003, n. 326*, Ordinanza del Presidente del Consiglio dei Ministri 8 luglio 2004, GU n. 165 del 16-7-2004. (in Italian)
- Park, S. and Mosalam, K.M. (2009), *Shear strength models of exterior beam-column joints without transverse reinforcement. PEER report 2009/106*, Pacific Earthquake Engineering Research Center, University of California, Berkeley.
- Paulay, T. and Priestley, M.J.N. (1992), *Seismic design of reinforced concrete and masonry buildings*, John Wiley & Sons Inc., New York, NY, USA.
- Regio Decreto n.2229 (1939), *Norme per la esecuzione delle opere in conglomerato cementizio semplice ed armato*, n.2229 del 16/11/1939. (in Italian)
- Santarella, L. (1963), *Prontuario del Cemento Armato. XXV Edizione*, U. Hoepli, Milano. (in Italian)
- Shin, M. and LaFave, J.M. (2004), "Seismic performance of reinforced concrete eccentric beam-column connections with floor slabs", *ACI Struct. J.*, **101**(3), 403-412.
- Sivaselvan, M.V. and Reinhorn, A.M. (2000), "Hysteretic models for deteriorating inelastic structures", *J. Eng. Mech.*, **126**(6), 633-640.
- Vecchio, F.J. and Collins, M.P. (1986), "The modified compression-field theory of reinforced concrete elements subjected to shear", *ACI Struct. J.*, **83**(2), 219-231.
- Vollum, R.L. and Newman, J.B. (1999), "The design of external,

reinforced concrete beam-column joints”, *Struct. Engineer*, **77**(23-24), 21-27.

Xing, G.H., Wu, T., Niu, D.T. and Liu, X. (2013), “Seismic behavior of reinforced concrete interior beam-column joints with beams of different depths”, *Earthq. Struct.*, **4**(4), 429-449.

Zhou, H. and Zhang, Z. (2012), “Interaction of internal forces of exterior beam-column joints of reinforced concrete frames under seismic action”, *Struct. Eng. Mech.*, **44**(2), 197-217.

SA